



A novel phosphine-free and recyclable palladium organic–inorganic hybrid magnetic nanocatalyst for Heck cross-coupling reactions

Maryam Barazandehdoust¹ · Manouchehr Mamaghani² · Hassan Kefayati¹

Received: 30 November 2019 / Accepted: 10 February 2020 / Published online: 21 February 2020
© Akadémiai Kiadó, Budapest, Hungary 2020

Abstract

A palladium organic–inorganic hybrid magnetic nanocatalyst for the Heck-cross coupling reactions was developed. This newly synthesized phosphine-free PdMNPs catalyzed Heck-cross coupling reactions in short reaction times (20–30 min) and high to excellent yields (75–93%). The catalyst was separated simply by an external magnet and reused in 10 successive runs without significant decrease in catalytic activity. The structure of the catalyst was established by Fourier transform infrared, X-ray diffraction, scanning electron microscopy, transmission electron microscopy, energy-dispersive X-ray spectroscopy, vibrating sample magnetometer and thermogravimetric analysis analyses.

Keywords Heck reaction · PdMNPs · Cross-coupling · Nanocatalyst · Palladium

Introduction

The Heck reaction or palladium-catalyzed arylation of olefins has received a prominent position among the transition metal catalyzed carbon–carbon bond forming in organic synthesis, in recent years. The Heck-cross coupling reactions are very broad in domain [1–6] and have been used in many areas such as molecular organic, natural products materials, polymers, pharmaceuticals, anti-oxidants, herbicides and industrial applications over the past few decades [7–11]. In most

Electronic supplementary material The online version of this article (<https://doi.org/10.1007/s11144-020-01744-5>) contains supplementary material, which is available to authorized users.

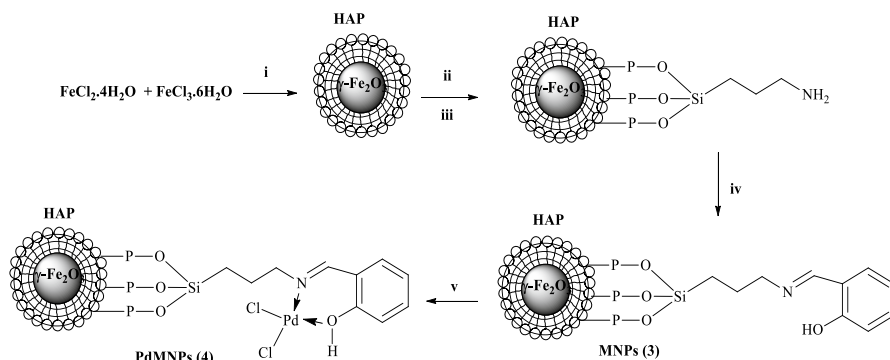
✉ Manouchehr Mamaghani
m-chem41@guilan.ac.ir

¹ Department of Chemistry, Faculty of Sciences, Islamic Azad University, Rasht Branch, P.O. Box 41335-3516, Rasht, Iran

² Department of Chemistry, Faculty of Sciences, University of Guilan, P.O. Box 41335-1914, Rasht, Iran

previous reports, the common ligands utilized for Heck-reactions are phosphine based. Since the phosphine ligands have several drawbacks such as difficulty of synthesis, expensive, toxic, air and/or moisture-sensitive, there has been great interest in developing phosphine free Pd catalyst for these reactions [12–18]. Palladium is a high-cost metal. Therefore, the development of easily accessible palladium catalyst for the Heck C–C coupling reaction, with high recyclability is a pivotal challenge for the synthetic chemists. The characteristics of ligand bonded to the Pd center play the most essential role in developing the reaction condition and high catalytic activity [19]. Furthermore, various catalysts utilized in the Heck-reaction are homogeneous which are faced with problems such as catalyst separation from the reaction concoction and furthermore the catalyst is not easily reused [20]. Recently, metal nanoparticles have gained considerable attentions in catalysis of organic reactions, in particular magnetic nanoparticles (MNPs) as a bridge between heterogeneous and homogenous catalysts are receiving more attentions due to high efficiency and simple recovery (green chemistry) from the reaction mixture by external magnetic field [21]. Therefore, eliminating the essential of tedious centrifugation and separation steps [22, 23]. To improve the chemical permanency as well as to attain some advantages such as the flexibility in surface modification, MNPs usually are coated with various organic or inorganic compounds, valuable metals and calcium hydroxyapatite $\text{Ca}_{10}(\text{PO}_4)_6(\text{OH})_3$ (HAP) [24–32]. In addition, covalently combining an active site onto a great surface area of a solid through a flexible spacer which makes an organic–inorganic hybrid catalyst is known as a way to simulate homogenous reaction conditions together having the advantage of reusability [20, 33–38].

In this work, we report palladium chloride supported on HAP-encapsulated- $\gamma\text{-Fe}_2\text{O}_3$ (designate as PdMNPs (4)) (Scheme 1) as an organic–inorganic hybrid super magnetic nanocatalyst for the Heck-reaction of aryl halides with various olefins under phosphine-free conditions.



Scheme 1 (i) $\text{Ca}(\text{NO}_3)_2$, $(\text{NH}_4)_2\text{HPO}_4$, NH_4OH , (ii) calcination, (iii) 3-aminopropyltrimethoxysilane, toluene, reflux, 48 h, (iv) 2-hydroxy benzaldehyde, dry EtOH, reflux, 24 h, and (v) PdCl_2 , EtOH, r.t., 12 h

Experimental

Apparatus and reagents

All materials were purchased from Merck and Fluka chemical companies and were used without any additional or further purification. The structures of MNP of Pd catalyst PdMNPs (**4**) were characterized by X-ray diffraction (XRD) (X-Pert MPD Philips diffractometer) with Co K_{α} ($\lambda = 1.7897 \text{ \AA}$) radiation. The thermal stability of the functionalized PdMNPs (**4**) was investigated by thermogravimetric analysis (TGA), differential scanning calorimetry (DSC) and differential thermal analysis (DTA). The thermogravimetric treatment of the specimen was scanned from 40 to 600 °C at the rate of 20 °C/min under Ar atmosphere by using TA-SDT Q600 instrument. $^1\text{H-NMR}$, and $^{13}\text{C-NMR}$ spectra were performed on a Bruker Advance 300 and 400 MHz spectrometers in CDCl_3 using TMS as the internal standard. Fourier transform infrared (FT-IR) spectra were recorded on a Shimadzu FT-IR 8900 spectrophotometer operating in transmission mode on KBr pellets. The IR spectra in Nujol was recorded on a Thermo scientific model Nicolet is10 (USA) FT-IR spectrophotometer. The amount of palladium was determined on an ICP Varian VISTA-PRO (400–4000) inductively coupled plasma optical emission (ICP-OES) with axial injection. The morphology of PdMNPs (**4**) was performed using a TESCAN Model MIRA3 XMU VP-FESEM variable pressure field emission scanning electron microscope (FESEM) with scanning range from 3 to 30 keV. The magnetization measurement was carried out in a vibrating sample magnetometer/alternating gradient force magnetometer (VSM/AGFM, MDK Co., Ltd., Iran). The magnetization curves of the nanocatalysis were obtained in an external field up to 15 T. TESCAN model MIRA3 with detector SAMX. Melting points were determined on an Electrothermal IA9100 series. The ultraviolet–visible absorption spectra were recorded in the range 200–800 nm using SCINCO S4100 UV–Vis spectrophotometer. UV–Vis spectrophotometer SCINCO S4100 with diffuse reflectance accessory (integrated sphere) was used for spectrophotometric measurements and transmission electron microscopy (TEM) analysis was carried out by a Philips CM120 transmission electron microscope, operating at accelerating voltage of 100 kV with 100 mesh TEM grid.

Synthesis of PdMNPs (**4**)

$[\gamma\text{-Fe}_2\text{O}_3\text{@HAp-Si-(CH}_2\text{)}_3\text{-NH}_2]$ was synthesized by the literature report [24, 39] with some modifications and then was allowed to react with equimolar amount of 2-hydroxybenzaldehyde in dry ethanol for 24 h under Ar atmosphere. Afterwards, the solid product was magnetically separated by an external magnet and eluted with dry ethanol to produce the catalyst MNPs (**3**) (Scheme 1). A stirring blend of catalyst MNPs (**3**) (0.47 g) and PdCl_2 (0.084 g) in ethanol (15 mL) was kept at room temperature for 12 h. The resultant light brown precipitate was filtered, washed repeatedly with ethanol, and dried under vacuum at room temperature to produce catalyst PdMNPs (**4**) (0.5 g).

General procedure for Heck cross-coupling

A mixture of aryl halide (1.0 mmol), olefin (1.5 mmol), TBAB (1 mmol, additive agent) PdMNPs (**4**) (0.0071 mmol), Et₃N (1.5 mmol) in DMF (2 mL) was stirred at 120 °C for 20 min. The progress of the reaction was monitored by TLC analysis. After the completion of the reaction, the catalyst was separated by an external magnet. Then, the catalyst was rinsed with DMF and resultant organic solution was evaporated under vacuum to produce a crude product which was purified by chromatography to furnish the desired products (Tables 2, 3, 4). The catalyst was washed by deionized water and EtOH (three times), dried at 100 °C and reused for the next run.

NMR data for the selected products

(E)-Methyl 3-(4-acetylphenyl) acrylate (**4a**)

Light-yellow solid, m.p. = 34–37 °C (lit. 32–36 °C [47]); FT-IR (KBr, cm⁻¹): 3045, 2959, 2922, 2854, 1713, 1686, 1551, 1427, 1097, 1036, 810; ¹H NMR (400 MHz, CDCl₃): δ_H = 8.0 (d, *J* = 8.4 Hz, 2H), 7.74 (d, *J* = 16.0 Hz, 1H), 7.64 (d, *J* = 8.4 Hz, 2H), 6.56 (d, *J* = 16.0 Hz, 1H), 3.86 (s, 3H), 2.65 (s, 3H); ¹³C (100 MHz, CDCl₃): δ_C = 197.4, 167.0, 143.3, 138.7, 138.0, 128.9, 128.2, 120.3, 52.0, 26.8.

(E)-Methyl 3-(4-methoxyphenyl)-2-methylacrylate (**4b**)

Pale-yellow oil (84%); FT-IR (KBr, cm⁻¹): 3010, 2954, 2842, 1708, 1604, 1444, 1309, 1251, 1180, 1177, 1027, 945, 827; ¹H NMR (300 MHz, CDCl₃): δ_H = 7.69 (s, 1H), 7.52 (d, *J* = 8.85 Hz, 2H), 6.92 (d, *J* = 8.85 Hz, 2H), 3.86 (s, 3H), 3.84 (s, 3H), 2.17 (d, *J* = 1.2 Hz, 3H); ¹³C (75 MHz, CDCl₃): δ_C = 170.5, 148.8, 137.7, 129.4, 127.4, 125.0, 112.9, 54.9, 52.0, 14.2.

(E)-Methyl 3-(4-acetylphenyl)-2-methylacrylate (**6b**)

Light-yellow solid (87%), m.p. = 80–82 °C; FT-IR (KBr, cm⁻¹): 3012, 2920, 2852, 1720, 1681, 1627, 1602, 1556, 1434, 1357, 1305, 1263, 1114, 956, 838; ¹H NMR (400 MHz, CDCl₃): δ_H = 7.98 (d, *J* = 8.0 Hz, 1H), 7.70 (s, 1H), 7.49 (d, *J* = 8.0 Hz, 1H), 3.73 (s, 3H), 2.63 (s, 3H), 2.13 (s, 3H); ¹³C (100 MHz, CDCl₃): δ_C = 196.8, 169.8, 141.5, 138.3, 136.4, 129.8, 128.6, 127.4, 53.3, 27.5, 14.2.

Result and discussion

Synthesis of PdMNPs (**4**)

PdMNPs were synthesized by the conventional co-precipitation method with some modifications [24, 40–43]. Initially, Fe₃O₄ nanoparticles were synthesized

by using $\text{FeCl}_2 \cdot 4\text{H}_2\text{O}$ and $\text{FeCl}_3 \cdot 6\text{H}_2\text{O}$ as starting materials and ammonia as a precipitating agent. Based on our previous report [41] after coating a layer of hydroxyapatite on the surface of the Fe_3O_4 nanoparticles and its calcinations at 400°C , it was functionalized by 3-aminopropyltrimethoxysilane to produce an organic–inorganic hybrid. Then, the prepared hybrid was reacted with 2-hydroxybenzaldehyde to produce a bi-dentate ligand for functionalized core–shell magnetic nanocatalyst. Finally, surface-bound ligands were complexed with palladium(II) by using PdCl_2 to furnish PdMNPs (**4**) (Scheme 1).

Characterization of PdMNPs (**4**)

X-ray diffraction (XRD)

The phase and crystallite structure of PdMNPs (**4**) were studied using XRD. The diffraction peaks appeared at $2\theta = 30.2^\circ$, 35.3° , 37.3° , 41.6° , 46.8° , 54.7° , 67.6° and 74.7° are related to the planes of (002), (220), (112), (311), (111), (200), (511) and (440) (Fig. 1), the resulted patterns can be referred to $\gamma\text{-Fe}_2\text{O}_3$ (JCPDS No. 39-1346) and hydroxyapatite (JCPDS No. 24-0033). No other phases were detected, indicating the phase purity of the sample. The average crystallite size of PdMNPs (**4**) sample was estimated from the most intense peak (111) using the Scherer formula [44]:

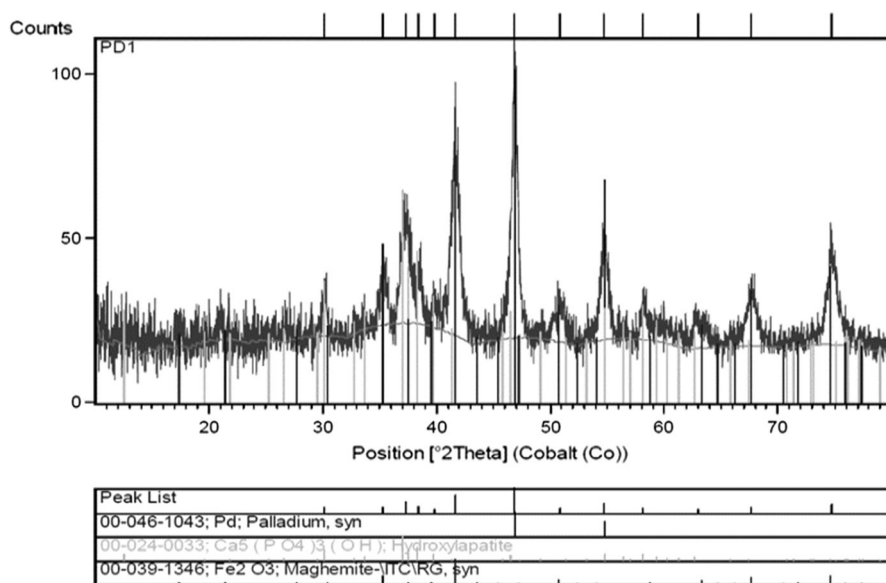


Fig. 1 The X-ray diffraction spectrum of the PdMNPs (**4**). Powder XRD analysis was carried out on a Philips X-Pert MPD diffractometer with $\text{Co K}\alpha$ ($\lambda = 1.7897 \text{ \AA}$) radiation at room temperature over 2 θ range 10° – 80° at a scan rate of $0.1^\circ/20\text{s}$

$$D_C = \frac{K\lambda}{\beta_{1/2} \cos \theta}$$

Here D_C is the crystallite diameter, K is the Scherrer constant (0.89), λ is the X-ray wavelength (0.15418 nm), and $\beta_{1/2}$ is the full width at half maximum of the diffraction peak and θ is the diffraction angle of the peak. The average crystallite size of PdMNPs (**4**) was estimated to be around 21.3 nm.

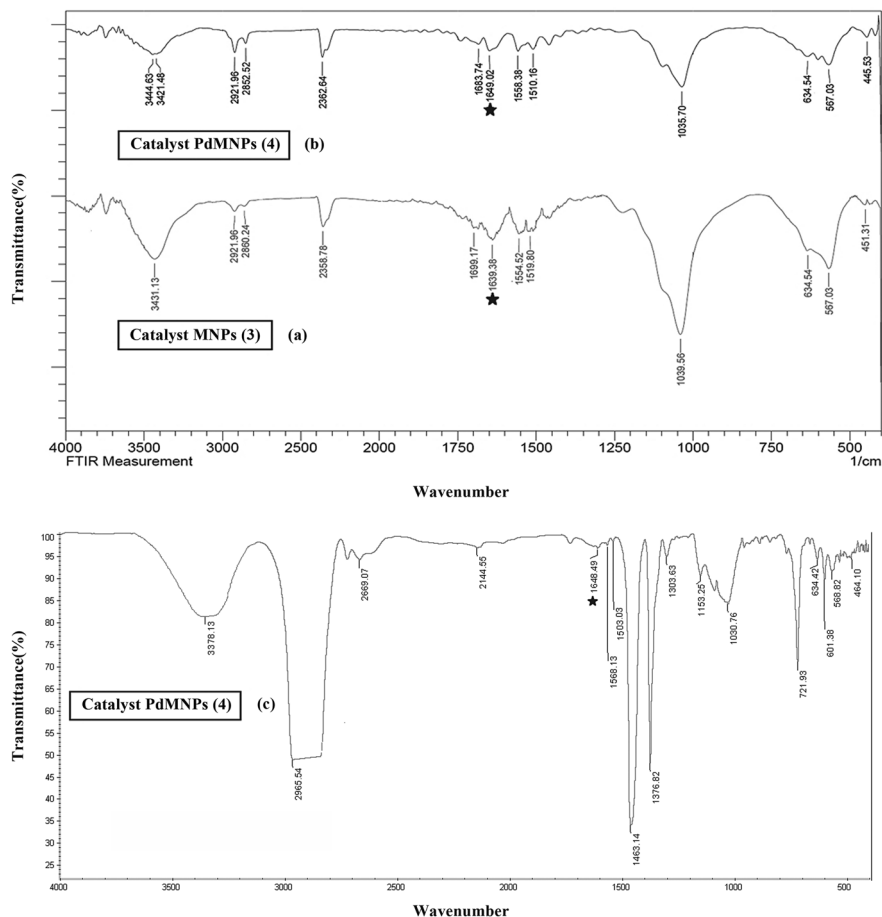


Fig. 2 FT-IR spectrum of the catalyst MNPs (**3**) and PdMNPs (**4**). The FT-IR spectra (**a**, **b**) of the samples were recorded on a Shimadzu FT-IR 8900 spectrophotometer operating in transmission mode on KBr pellets. The samples were mixed with KBr and compressed into a pellet and placed into an IR cell. The spectra were recorded in the range of 400–4000 cm^{-1} with a resolution of 4 cm^{-1} at room temperature. Spectrum **c** was recorded in nujol

Fourier-transform infrared spectroscopy (FT-IR)

FT-IR spectrum of the prepared nanocatalyst is shown in Fig. 2b (in KBr). The absorption peak at 445 cm^{-1} can be assigned to the Fe–O absorption in the maghemite [45]. The O–P–O surface phosphate groups in the hydroxyapatite shell emerged at 567 and 604 cm^{-1} which were in overlap with Fe–O stretching. The P–O stretching emerged at 1035 cm^{-1} . The bands at around 1510 and 1558 cm^{-1} are associated to the aromatic C=C stretching also a band at 1649 cm^{-1} produced by C=N double bond, verify that the organic linker exactly immobilized onto the surface. Note that the C=N band is shifted to a higher wave number compared to the C=N stretching frequency of MNPs (3) (Fig. 2a) (1649 cm^{-1} rather than 1639 cm^{-1}). It is implying that C=N and OH groups are coordinated to Pd through the lone pair of N and O. FT-IR spectrum of the catalyst was also recorded in nujol (Fig. 2c). The bands related to OH (3378 cm^{-1}) and C=N (1648 cm^{-1}) groups of the ligand are evident in the spectra.

Scanning electron microscopy (SEM)

The morphology and particle size of the PdMNPs were investigated by SEM micrograph (Fig. 3). The micrograph shows that the catalyst obviously showed the nano size of the particles and possesses a spherical shape. Also, the average size of the PdMNPs is around 23 nm (Fig. 3a, b) which is in good agreement with that of estimated by Scherrer's equation from XRD spectrum. Fig. 3c shows the presence of Pd in catalyst PdMNPs (4). The SEM image of the catalyst proved that after ten consecutive runs of the reaction, no change occurred in the shape and size of the nanoparticles (Fig. 3d).

The ICP-AES analysis was utilized for accurate determination of the palladium content in the synthesized PdMNPs (4). Analysis verified $0.71\text{ mmol Pd g}^{-1}$ (7.54%) of the PdMNPs which is in consensus with the EDS consequence.

Energy-dispersive X-ray spectroscopy (EDS)

EDS analysis spectrum for PdMNPs (4) presented in Fig. 4 reveals the existence of palladium in the structure. As is obvious from the Fig. 4 Ca, P, Fe, Si, Pd and Cl associated to the nanocatalyst structure, are seen in the spectrum. The proportion of palladium: chlorine: nitrogen in the spectrum is observed to be 4.03:1:2.15. The amount of palladium in the synthesized PdMNPs is 7.35% according to the EDS analysis, which is equivalent to 0.69 mmol of palladium per gram of PdMNPs.

Vibrating sample magnetometer (VSM)

The magnetic property of the PdMNPs was studied using VSM technique (Fig. 5). Fig. shows the hysteresis loop of the PdMNPs at room temperature as the external magnetic field was changed from -10 to 10 KOe ($-10,000$ to $10,000\text{ Oe}$). For super paramagnetic particles, the magnetization becomes zero when the external field approached zero. As it can be seen (Fig. 5) the hysteresis curve of PdMNPs

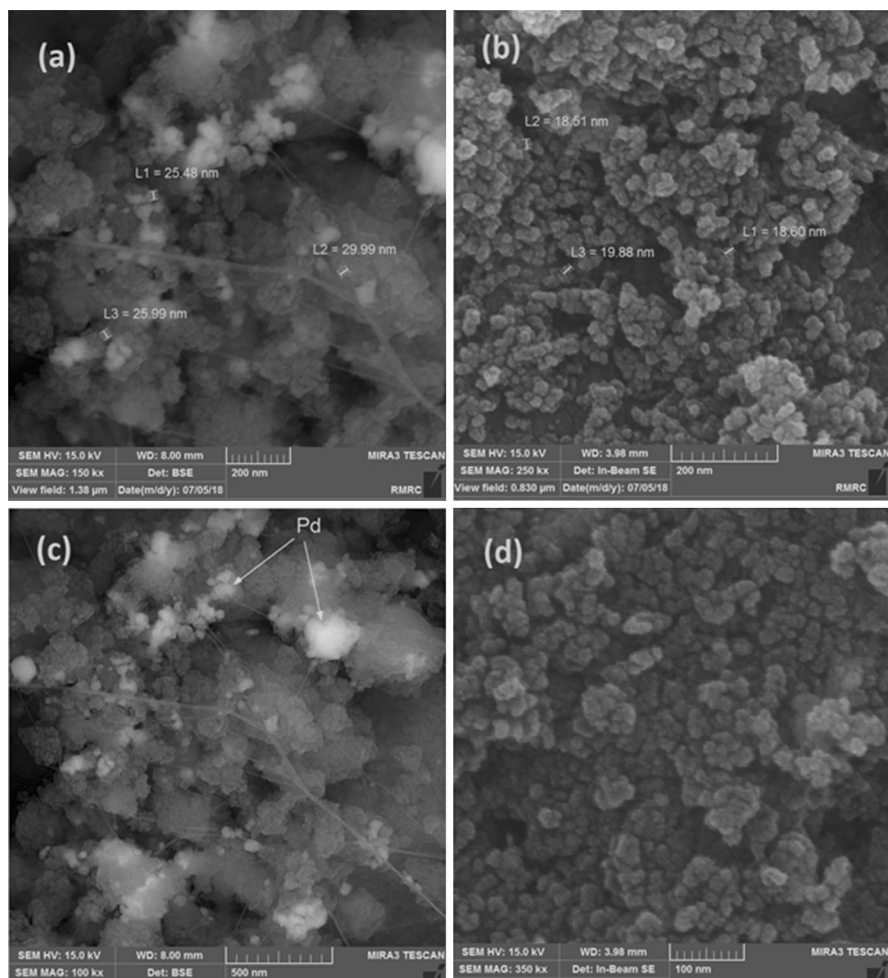


Fig. 3 SEM image of the PdMNPs (**4**) (**a**, **b**) (nano particles with average size of 23 nm), SEM image shows the presence of palladium in MNPs (**c**), SEM image (after 10th cycle of the reaction) of the PdMNPs (**4**) (**d**). Scanning electron microphotographs (SEM) were recorded by using a TESCAN Model MIRA3 XMU VP-FESEM variable pressure field emission scanning electron microscope (FESEM) with scanning range from 3 to 30 keV and an Au layer coating on carbon support

passed through the zero point of magnetization which confirms its super paramagnetic nature. The saturation magnetization (M_s) value of the synthesized PdMNPs is estimated to be approximately 24.65 emu g^{-1} .

Thermogravimetric analysis (TGA)

The thermal analysis method is a potent tool for characterizing a system (element, compound or mixture) by measuring changes in physico-chemical properties at high temperatures as a function of increasing temperature. Thermal stability of PdMNPs

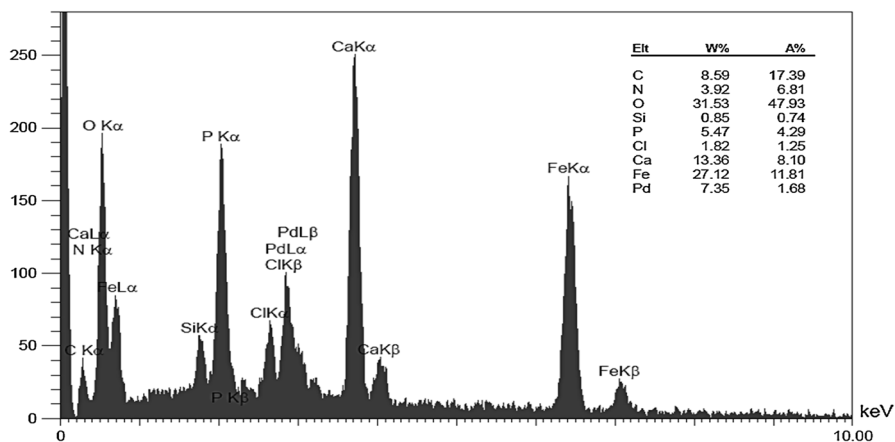


Fig. 4 EDS spectrum of the PdMNPs (4). The amount of palladium was determined on an ICP Varian VISTA-PRO (400–4000) inductively coupled plasma optical emission (ICP-OES) with axial injection

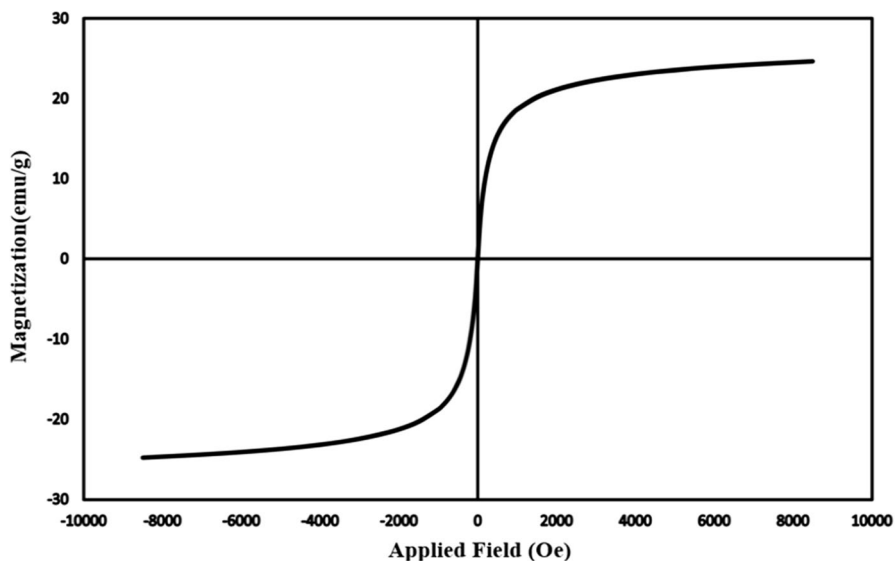


Fig. 5 Magnetization (M) as a function of field (H) for PdMNPs (4). The magnetization measurement was carried out in a vibrating sample magnetometer/alternating gradient force magnetometer (VSM/AGFM, MDK Co., Ltd., Iran). The magnetization curves of the nanocatalysis were obtained in an external field up to 15 T ESCAN model MIRA3 with detector SAMX

(4) were performed by thermo gravimetric analysis (TGA), Differential thermal analyzer (DTA) and Differential scanning calorimetric (DSC) analyzer (Fig. 6). TGA with heating in a range altering from room temperature to 600 °C showed weight loss of 11.96%, which could be presumably related to the evaporation of the external water and decomposition of organic groups situated on the surface of PdMNPs (4).

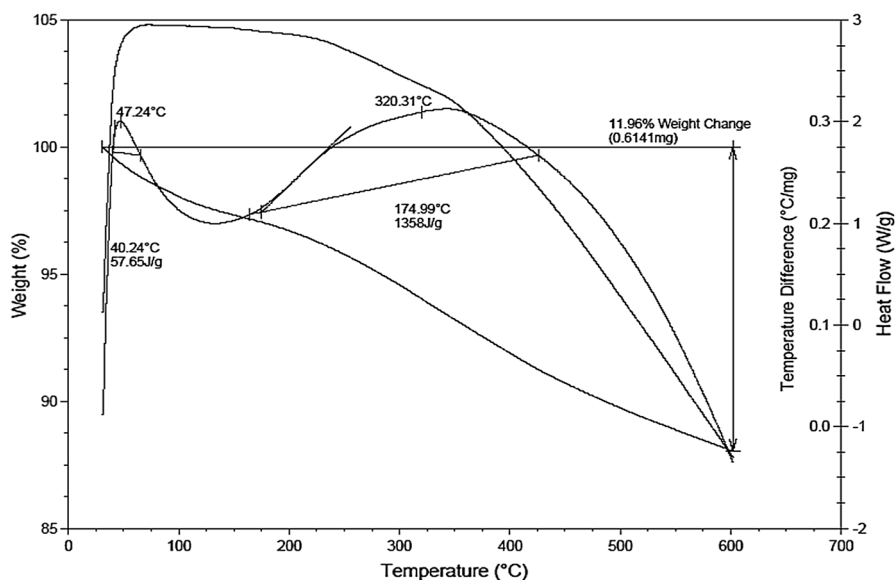


Fig. 6 Total thermogram of the PdMNPs (**4**). Thermogravimetric analysis (TGA), differential scanning calorimetry (DSC) and differential thermal analysis (DTA) were measured by using TA-SDT Q600 instrument scanning from 40 to 600 °C at the rate of 20 °C/min under Ar atmosphere

Diffuse reflection spectrometry analysis (DRS)

A different verification of permanency of PdMNPs (**4**) showed approximately the same diffuse reflectance spectra (DRS) before and after being used in the model reaction (Fig. 7). The experiments showed that PdMNPs (**4**) at high temperature were significantly remained constant without any changes. It is noteworthy that the PdMNPs (**4**) did not change much in catalysts weight and the efficiency of the products even after 10 times recovery. This fact is indicative of strong bonding between MNPs and palladium which lends support to the postulate of covalent bonds between these two components.

Transmission electron microscopy (TEM)

TEM analysis of PdMNPs (**4**) is shown in Fig. 8a. The presence of ashy maghemite seeds that partially covered the smooth clusters of nanocatalyst is clear from the TEM. According to TEM image, the black palladium colloidal particles are well dispersed through the catalyst surface in average size distribution of 16.8 nm (Fig. 8b).

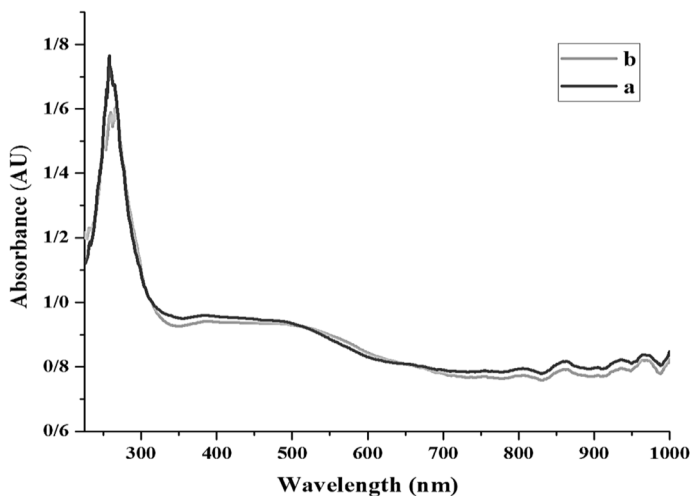


Fig. 7 UV–Vis DRS spectra of PdMNPs (**4**) before (a) and after (b) using 10 consecutive runs in the model reaction. The ultraviolet–visible absorption spectra were recorded in the range 200–800 nm by using SCINCO S4100 UV–Vis spectrophotometer with diffuse reflectance accessory (integrated sphere)

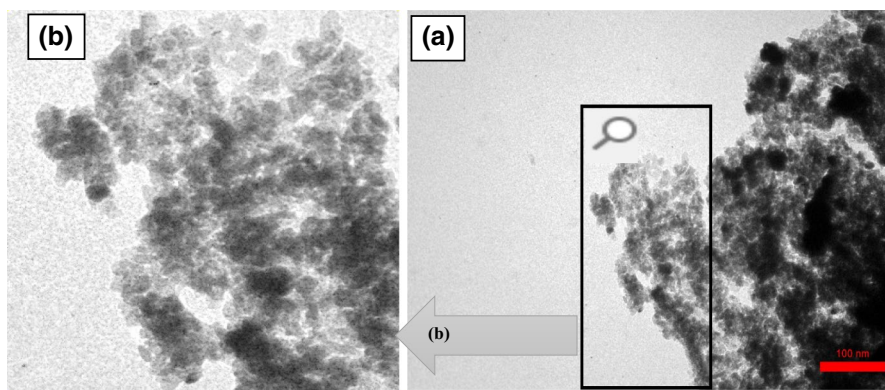
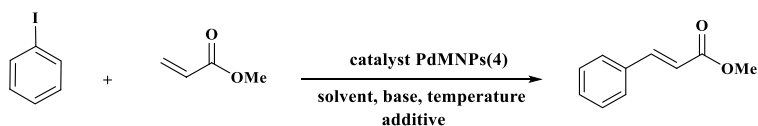


Fig. 8 a and b TEM micrographs of PdMNPs (**4**). TEM analysis was recorded using Philips CM120 microscope, operated with a 100 kV accelerating voltage with 100 mesh TEM grid

Catalytic activity of PdMNPs (**4**) for the Heck-reactions

The Heck-coupling reaction of iodobenzene with methyl acrylate was chosen as the model reaction to evaluate the potential catalytic activity of PdMNPs (**4**). The optimization was performed with respect to solvent, base, temperature and additive by using PdMNPs as catalyst (Table 1). Due to the fact that in Heck reactions polar aprotic solvents are commonly used, H₂O, DMF, THF and EtOH/H₂O solvents were selected. Among the solvents selected for the coupling reactions, DMF was preferred as the solvent of choice. When TBAB was added to the reaction

Table 1 Optimization of the reaction parameters

Entry	Solvent	Base	Temperature (°C)	Additive	Time	Yield ^a (%)
1	H ₂ O	Et ₃ N	100	TBAB	20 min	NR
2	Toluene	Et ₃ N	110	TBAB	20 min	60
3	THF	Et ₃ N	65	TBAB	20 min	35
4	EtOH/H ₂ O	Et ₃ N	80	TBAB	20 min	NR
5	DMF	Et ₃ N	120	TBAB	25 min	93
6	DMF	Et ₃ N	120	TBAB	20 min	93
7	DMF	Et ₃ N	120	TBAB	15 min	85
8	DMF	Et ₃ N	120	–	20 min	NR
9	DMF	Et ₃ N	100	TBAB	20 min	75
10	DMF	Et ₃ N	50	TBAB	20 min	30
11	DMF	Et ₃ N	r.t.	TBAB	20 min	NR
12	DMF	Na ₂ CO ₃	120	TBAB	20 min	78
13	DMF	K ₂ CO ₃	120	TBAB	20 min	85
14	DMF	K ₃ PO ₄	120	TBAB	20 min	64
15	DMF	Bu ₄ NOH	120	TBAB	20 min	NR

Reaction conditions: iodobenzene (1.0 mmol), methyl acrylate (1.5 mmol), base (1.5 mmol), PdMNPs (4) (10 mg, 0.71 mol%), solvent (2 mL), TBAB (1 mmol)

^aIsolated yields after purification by chromatography

in DMF, showed high selectivity for the *trans*-isomer products in all cases, and no *cis* products were observed. It should be noted that DMF plays a role as an appropriate polar solvent and a reducing agent for converting Pd(II) to Pd(0) to perform carbon–carbon coupling reactions the postulate which is also supported by the literature report [46]. Among the selected bases Na₂CO₃, K₂CO₃, Et₃N, K₃PO₄ and Bu₄NOH, organic base Et₃N had the highest and K₃PO₄ the lowest yield and Bu₄NOH no product. The investigations at different temperature within 50–120 °C were performed for the model reaction, which eventually 120 °C was chosen as optimal temperature. Under the optimized conditions by using DMF and Et₃N at 120 °C the reaction times were diversified to get the quantitative yield of product within 20 min for the reaction of iodobenzene and methyl acrylate (Table 1, Entry 6). The coupling reaction of iodobenzene and methyl acrylate did not proceed in the absence of TBAB (Table 1, Entry 8). However, the addition of 1 mmol TBAB/mmol substrate, furnished the desired product in

excellent yield. TBAB as additive sustains palladium nanoparticles stability and therefore enhances its activity.

Obtaining an impressive result in the PdMNPs (4) catalyzed Heck-reaction of iodobenzene with methyl acrylate under optimization condition (Table 1, Entry 6), the protocol was applied to different palladium-catalyzed coupling reactions of aryl halides carrying either electron-donating or electron withdrawing groups in aromatic rings with terminal olefins (methyl acrylate, methyl methacrylate, *n*-butyl acrylate and vinyl acetate (Table 2). In all cases, the *trans*-products were selectively produced with no detectable trace of *cis*-isomer. As shown in Table 2, all products were obtained in short reaction times and high to excellent yields in the presence of PdMNPs (4).

A comparison of the efficiency of present PdMNPs (4) catalyst and some heterogeneous and homogenous palladium catalysts is given in Table 3. Evidently, the present catalyst is superior in terms of reaction time, TON and recyclability (Table 3, Entry 6). As it is clear from the results this work prevail over drawbacks of some other works such as longer reaction time, difficult reaction conditions and elimination of phosphine ligands.

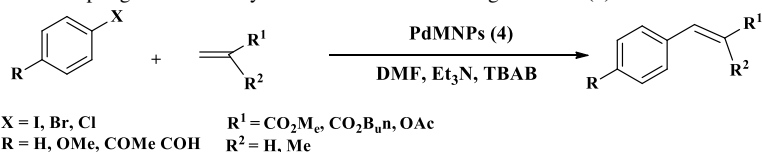
The optimized amount of catalyst for the model reaction was found to be 0.71 mol%. A decrease in the amount of nanocatalyst reduced the yield but an increase in its amount did not have any appreciable effect on the overall yield of product (Table 4).

Recyclability of the catalyst

After completion of the reaction, the PdMNPs (4) was separated from the reaction mixture by an external magnet and washed several times with DMF to ensure that all the products were separated from the nanoparticles. The residue was washed three times with deionized water and ethanol for further purification and finally, dried at 100 °C in the oven and used in the next run. Recyclability of the catalyst for the model reaction is shown in Fig. 9. The catalytic system exhibited a remarkable activity and maintained its catalytic performance during 10 successive cycles without perceptible reduction in the catalytic activity.

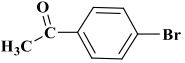
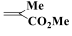
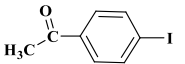
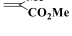
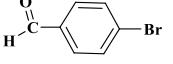

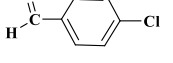
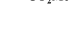
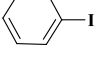

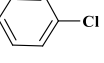

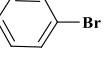
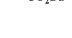
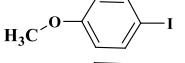
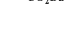
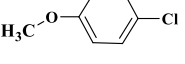
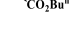
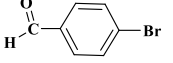
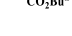
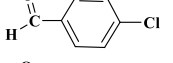

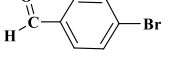

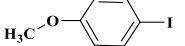

Conclusion

A novel heterogeneous HAp-encapsulated- γ -Fe₂O₃-based Pd(II) organic–inorganic hybrid nanocatalyst was prepared and was used in the Heck cross-coupling reaction. This practical method gives rapid access to a range of Heck products under low palladium loadings, in lower reaction time and high to excellent yields. The catalyst is stable towards air and moisture and easily handled without any special precautionary measures and also benefits from several more advantages such as, easy recovery from the reaction system by using an external magnet, high recyclability in which 10 reuses did not result in appreciable decrease in its catalytic activities and avoiding the use of phosphine ligands.

Table 2 Heck coupling reaction of aryl halides with olefins using PdMNPs (4)

Entry	Aryl halide	Alkenes	Yield ^{b, c} (%)	M.P (°C)		TON ^d
				Observed	Reported	
1a		$\text{CH}_2=\text{CO}_2\text{Me}$	93	122-124	122-123 [47]	131
2a		$\text{CH}_2=\text{CO}_2\text{Me}$	83	34-36	32-36 [48]	117
3a		$\text{CH}_2=\text{CO}_2\text{Me}$	79	35-37	32-36 [48]	111
4a		$\text{CH}_2=\text{CO}_2\text{Me}$	90	34-37	32-36 [48]	127
5a		$\text{CH}_2=\text{CO}_2\text{Me}$	88	123-125	122-123 [47]	124
6a		$\text{CH}_2=\text{CO}_2\text{Me}$	86	121-124	122-123 [47]	121
7a		$\text{CH}_2=\text{CO}_2\text{Me}$	91	82-86	84-86 [48]	128
8a		$\text{CH}_2=\text{CO}_2\text{Me}$	87	83-87	84-86 [48]	122
9a		$\text{CH}_2=\text{CO}_2\text{Me}$	76	82-85	82-84 [48]	107
10a		$\text{CH}_2=\text{CO}_2\text{Me}$	80	81-84	82-84 [48]	112
1b		$\text{CH}_2=\text{C}(\text{Me})\text{CO}_2\text{Me}$	88	Pale yellow-oil	Oil [49]	124
2b		$\text{CH}_2=\text{C}(\text{Me})\text{CO}_2\text{Me}$	82	Pale yellow-oil	Pale yellow-oil[50]	115
3b		$\text{CH}_2=\text{C}(\text{Me})\text{CO}_2\text{Me}$	80	Pale yellow-oil	-	112
4b		$\text{CH}_2=\text{C}(\text{Me})\text{CO}_2\text{Me}$	84	Pale yellow-oil	-	118
5b		$\text{CH}_2=\text{C}(\text{Me})\text{CO}_2\text{Me}$	86	Pale yellow-oil	-	121

Table 2 (continued)

6b			87	80-82	-	122
7b			89	79-81	-	125
8b			80	Colorless oil	Oil [50]	112
9b			76	Colorless oil	Oil [50]	107
1c			90	Colorless oil	Oil [51]	126
2c			85	Colorless oil	Oil [49]	119
3c			88	Colorless oil	Oil [51]	124
4c			91	Colorless oil	Oil [51]	128
5c			88	Colorless oil	Oil [51]	124
6c			82	106-109	108-109[52]	115
7c			80	106-107	108-109[52]	112
1d			72	Colorless oil	Oil [53]	101
2d			53	Colorless oil	Oil [53]	74

Reaction conditions: aryl halide (1.0 mmol), alkene (1.5 mmol), Et₃N (1.5 mmol), PdMNPs (**4**) (10 mg, 0.71 mol%), DMF (2 mL), TBAB (1 mmol) added, at 120 °C

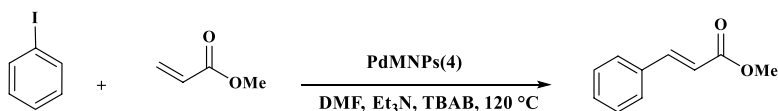
^bIsolated yields after TLC purification by silica gel plates

^bReaction times 20–30 min

^cTurn over number (TON) based on the number of mole of isolated product

Table 3 Comparison of PdMNPs (**4**) catalyst with some heterogeneous and homogeneous catalysts for the Heck reaction of iodobenzene and methyl acrylate

Entry	Catalyst	Loading	Time	Yield (%)	Reusability	References
1	Catalyst I-Pd	300 mg	24 h	90	No	[54]
2	PdNP/ α -ZrPK	0.1 mol%	3 h	98	6 Cycles	[55]
3	SBA-TMG-Pd	0.01 mol%	65 min	91	7 Cycles	[49]
4	Pd(OAc) ₂	4.45 mol%	6 h	78	No	–
5	PdCl ₂	5.63 mol%	12 h	62	No	–
6	PdMNPs (4)	0.71 mol%	20 min	93	Successful in 10 cycles	This work

Table 4 Optimization the amount of applied supported PdMNPs (**4**) in the model reaction

Entry	PdMNPs (mg, mol%)	Time (min)	TON ^a	Yield ^b (%)
1	None	20	–	NR
2	15, 1.1	20	85	94
3	10, 0.71	20	131	93
3	7, 0.5	20	170	85
4	5, 0.36	20	222	80

Reaction conditions: iodobenzene (1.0 mmol), methyl acrylate (1.5 mmol), Et₃N (1.5 mmol), PdMNPs (**4**) (as table), DMF (2 mL), TBAB (1 mmol), 120 °C

^aTurn over number (TON) based on the number of mole of isolated product

^bIsolated yields after TLC purification by silica gel plates

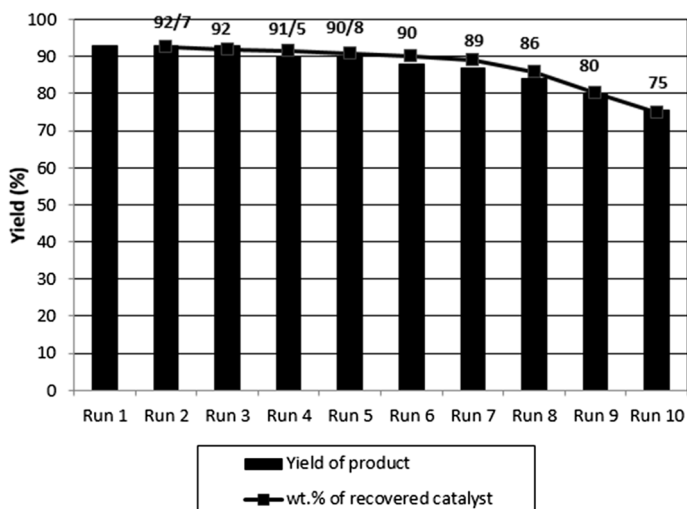


Fig. 9 Recyclability of PdMNPs (**4**) in the model reaction. Reaction conditions: iodobenzene (1.0 mmol), methyl acrylate (1.5 mmol), Et₃N (1.5 mmol), PdMNPs (**4**) (10 mg, 0.71 mol%), DMF (2 mL), TBAB (1 mmol), 120 °C

References

- Karimi B, Enders D (2006) New *N*-heterocyclic carbene palladium complex/ionic liquid matrix immobilized on silica: application as recoverable catalyst for the Heck reaction. *Org Lett* 8:1237–1240
- Prakash GKS, Krishnan HS, Jog PV, Iyer AP, Olah GA (2012) A domino approach of Heck coupling for the synthesis of β -trifluoromethylstyrenes. *Org Lett* 14:1146–1149
- de Meijere A, Meyer Frank E (1995) Fine feathers make fine birds: the Heck reaction in modern garb. *Angew Chem Int Ed* 33:2379–2411
- Heck RF (1991) In: Trost MB (ed) *Comprehensive organic synthesis*. Elsevier, New York
- Beletskaya IP, Cheprakov AV (2000) The Heck reaction as a sharpening stone of palladium catalysis. *Chem Rev* 100:3009–3066
- de Meijere A, Bräse S (2004) *Metal-catalyzed cross-coupling reactions*. Wiley-VCH, New York
- Pratihari JL, Pattanayak P, Patra D, Lin C-H, Chattopadhyay S (2012) Synthesis, characterization and structure of new diazoketiminato chelates of palladium(II): potential catalyst for C-C coupling reactions. *Polyhedron* 33:67–73
- Aydemir M, Durap F, Baysal A, Akba O, Gümüş B, Özkar S, Yıldırım LT (2009) Synthesis and characterization of new bis(diphenylphosphino)aniline ligands and their complexes: X-ray crystal structure of palladium(II) and platinum(II) complexes, and application of palladium(II) complexes as pre-catalysts in Heck and Suzuki cross-coupling reactions. *Polyhedron* 28:2313–2320
- Chen X, Engle Keary M, Wang D-H, Yu J-Q (2009) Palladium(II)-catalyzed C-H activation/C–C cross-coupling reactions: versatility and practicality. *Angew Chem Int Ed* 48:5094–5115
- Barnard BC (2008) *Platin Met Rev* 52:38–45
- Röhlich C, Köhler K (2010) Macrocyclic palladium(II) complexes in C-C coupling reactions: efficient catalysis by controlled temporary release of active species. *Adv Synth Catal* 352:2263–2274
- García-Melchor M, Fuentes B, Lledós A, Casares JA, Ujaque G, Espinet P (2011) Cationic intermediates in the Pd-catalyzed Negishi coupling. Kinetic and density functional theory

- study of alternative transmetalation pathways in the Me–Me coupling of ZnMe_2 and *trans*-[PdMeCl(PMePh₂)₂]. *J Am Chem Soc* 133:13519–13526
13. Borah BJ, Saikia K, Saikia PP, Barua NC, Dutta DK (2012) PdO-nanoparticles stabilized by tripodal phosphine based ligands and their catalytic activities on carbon-carbon bond formation reactions. *Catal Today* 198:174–183
 14. Slagt VF, de Vries AHM, de Vries JG, Kellogg RM (2010) Practical aspects of carbon-carbon cross-coupling reactions using heteroarenes. *Org Process Res Dev* 14:30–47
 15. Morgan BP, Galdamez GA, Gilliard JR Jr, Smith RC (2009) Canopied *trans*-chelating bis(*N*-heterocyclic carbene) ligand: synthesis, structure and catalysis. *Dalton Trans.* <https://doi.org/10.1039/B815739A>
 16. Bakherad M, Keivanloo A, Bahramian B, Jajarmi S (2010) Copper- and solvent-free Sonogashira coupling reactions of aryl halides with terminal alkynes catalyzed by 1-phenyl-1,2-propanedione-2-oxime thiosemi-carbazone-functionalized polystyrene resin supported Pd(II) complex under aerobic conditions. *Appl Catal A* 390:135–140
 17. Alizadeh A, Khodaei MM, Kordestani D, Beygzadeh M (2013) Highly efficient phosphine-free Suzuki aryl couplings mediated by an in situ generated Pd(OAc)₂/metformin complex in green media. *Tetrahedron Lett* 54:291–294
 18. Yang Q, Wu H, Zhan H, Hou J, Gao M, Su Q, Wu S (2020) Attapulgite-anchored Pd complex catalyst: a highly active and reusable catalyst for C-C coupling reactions. *React Kinet Mech Cat.* <https://doi.org/10.1007/s11144-019-01698-3>
 19. Johansson Seechurn Carin CC, Kitching Matthew O, Colacot Thomas J, Snieckus V (2012) Palladium-catalyzed cross-coupling: a historical contextual perspective to the 2010 Nobel Prize. *Angew Chem Int Ed* 51:5062–5085
 20. Lu Z-L, Lindner E, Mayer HA (2002) Applications of sol-gel-processed interphase catalysts. *Chem Rev* 102:3543–3578
 21. Kidwai M, Jain A, Bhardwaj S (2012) Magnetic nanoparticles catalyzed synthesis of diverse *N*-heterocycles. *Mol Divers* 16:121–128
 22. Phan Nam TS, Gill Christopher S, Nguyen Joseph V, Zhang ZJ, Jones Christopher W (2006) Expanding the utility of one-pot multistep reaction networks through compartmentation and recovery of the catalyst. *Angew Chem Int Ed* 45:2209–2212
 23. Abu-Reziq R, Alper H, Wang D, Post ML (2006) Metal supported on dendronized magnetic nanoparticles: highly selective hydroformylation catalysts. *J Am Chem Soc* 128:5279–5282
 24. Ma'mani L, Sheykhani M, Heydari A, Faraji M, Yamini Y (2010) Sulfonic acid supported on hydroxyapatite-encapsulated- γ -Fe₂O₃ nanocrystallites as a magnetically Brønsted acid for *N*-formylation of amines. *Appl Catal A* 377:64–69
 25. Teunissen W, Bol AA, Geus JW (1999) Magnetic catalyst bodies. *Catal Today* 48:329–336
 26. Yoon T-J, Lee W, Oh Y-S, Lee J-K (2003) Magnetic nanoparticles as a catalyst vehicle for simple and easy recycling. *N J Chem* 27:227–229
 27. Yoon H, Ko S, Jang J (2007) Nitrogen-doped magnetic carbon nanoparticles as catalyst supports for efficient recovery and recycling. *Chem Commun* 38(14):1468–1470
 28. Yang H-H, Zhang S-Q, Chen X-L, Zhuang Z-X, Xu J-G, Wang X-R (2004) Magnetite-containing spherical silica nanoparticles for biocatalysis and bioseparations. *Anal Chem* 76:1316–1321
 29. Lee D, Lee J, Lee H, Jin S, Hyeon T, Kim BM (2006) Filtration-free recyclable catalytic asymmetric dihydroxylation using a ligand immobilized on magnetic mesocellular mesoporous silica. *Adv Synth Catal* 348:41–46
 30. Zhang Y, Li Z, Sun W, Xia C (2008) A magnetically recyclable heterogeneous catalyst: cobalt nanoxide supported on hydroxyapatite-encapsulated γ -Fe₂O₃ nanocrystallites for highly efficient olefin oxidation with H₂O₂. *Catal Commun* 10:237–242
 31. Deng J, Mo L-P, Zhao F-Y, Hou L-L, Yang L, Zhang Z-H (2011) Sulfonic acid supported on hydroxyapatite-encapsulated-[gamma]-Fe₂O₃ nanocrystallites as a magnetically separable catalyst for one-pot reductive amination of carbonyl compounds. *Green Chem* 13:2576–2584
 32. Liu Y-H, Deng J, Gao J-W, Zhang Z-H (2012) Triflic acid-functionalized silica-coated magnetic nanoparticles as a magnetically separable catalyst for synthesis of gem-dihydroperoxides. *Adv Synth Catal* 354:441–447
 33. Baleizao C, Corma A, Garcia H, Leyva A (2003) An oxime-carbapalladacycle complex covalently anchored to silica as an active and reusable heterogeneous catalyst for Suzuki cross-coupling in water. *Chem Commun.* <https://doi.org/10.1039/B211742H>

34. Wang D, Astruc D (2014) Fast-growing field of magnetically recyclable nanocatalysts. *Chem Rev* 114:6949–6985
35. Stevens PD, Li G, Fan J, Yen M, Gao Y (2005) Recycling of homogeneous Pd catalysts using superparamagnetic nanoparticles as novel soluble supports for Suzuki, Heck, and Sonogashira cross-coupling reactions. *Chem Commun*. <https://doi.org/10.1039/B505424A>
36. Dálaigh CÓ, Corr Serena A, Gunko Y, Connon Stephen J (2007) N-dialkylaminopyridine catalyst: excellent reactivity combined with facile catalyst recovery and recyclability. *Angew Chem Int Ed* 46:4329–4332
37. Wight AP, Davis ME (2002) Design and preparation of organic–inorganic hybrid catalysts. *Chem Rev* 102:3589–3614
38. Tabatabaieian K, Zanjanchi MA, Mamaghani M, Dadashi A (2016) Diversity oriented synthesis of benzoxanthene and benzochromene libraries via one-pot, three-component reactions and their anti-proliferative activity. *Res Chem Intermed* 42:5049–5067
39. Khoobi M, Ma'mani L, Rezaazadeh F, Zareie Z, Foroumadi A, Ramazani A, Shafiee A (2012) One-pot synthesis of 4*H*-benzo[*b*]pyrans and dihydropyrano[*c*]chromenes using inorganic–organic hybrid magnetic nanocatalyst in water. *J Mol Catal A* 359:74–80
40. Sheykhani M, Mohammadquli M, Heydari A (2012) A new and green synthesis of formamidines by $\gamma\text{-Fe}_2\text{O}_3\text{@SiO}_2\text{-HBF}_4$ nanoparticles as a robust and magnetically recoverable catalyst. *J Mol Struct* 1027:156–161
41. Mohsenimehr M, Mamaghani M, Shirini F, Sheykhani M, Moghaddam FA (2014) One-pot synthesis of novel pyrido[2,3-*d*]pyrimidines using HAp-encapsulated- $\gamma\text{-Fe}_2\text{O}_3$ supported sulfonic acid nanocatalyst under solvent-free conditions. *Chin Chem Lett* 25:1387–1391
42. Ma'mani L, Sheykhani M, Heydari A (2011) Nanosilver embedded on hydroxyapatite-encapsulated $\gamma\text{-Fe}_2\text{O}_3$: superparamagnetic catalyst for chemoselective oxidation of primary amines to *N*-monoalkylated hydroxylamines. *Appl Catal A* 395:34–38
43. Sheykhani M, Ma'mani L, Ebrahimi A, Heydari A (2011) Sulfamic acid heterogenized on hydroxyapatite-encapsulated $\gamma\text{-Fe}_2\text{O}_3$ nanoparticles as a magnetic green interphase catalyst. *J Mol Catal A* 335:253–261
44. Cullity BD (1956) *Elements of X ray diffraction*. Addison-Wesley Publishing Company, London
45. Sabu Thomas KJ, Malhotra SK, Koichi G, Sreekala MS (2013) *Polymer composites, nanocomposites*. Wiley-VCH, Weinheim
46. Pastoriza-Santos I, Liz-Marzán LM (2009) *N*-dimethylformamide as a reaction medium for metal nanoparticle synthesis. *Adv Funct Mater* 19:679–688
47. Hajipour Abdol R, Karami K, Pirisedigh A (2009) Accelerated Heck reaction using *ortho*-palladated complex with controlled microwave heating. *Appl Organomet Chem* 23:504–511
48. Hajipour AR, Karami K, Pirisedigh A, Ruoho AE (2009) Application of dimeric orthopalladate complex of homoveratrylamine as an efficient catalyst in the Heck cross-coupling reaction. *J Organomet Chem* 694:2548–2554
49. Ma X, Zhou Y, Zhang J, Zhu A, Jiang T, Han B (2008) Solvent-free Heck reaction catalyzed by a recyclable Pd catalyst supported on SBA-15 via an ionic liquid. *Green Chem* 10:59–66
50. Wu S, Ma H, Jia X, Zhong Y, Lei Z (2011) Biopolymer–metal complex wool–Pd as a highly active heterogeneous catalyst for Heck reaction in aqueous media. *Tetrahedron* 67:250–256
51. Firouzabadi H, Iranpoor N, Ghaderi A (2011) Solvent-free Mizoroki–Heck reaction catalyzed by palladium nano-particles deposited on gelatin as the reductant, ligand and the non-toxic and degradable natural product support. *J Mol Catal A* 347:38–45
52. Xu H-J, Zhao Y-Q, Zhou X-F (2011) Palladium-catalyzed Heck reaction of aryl chlorides under mild conditions promoted by organic ionic bases. *J Org Chem* 76:8036–8041
53. Meng L, Liu C, Zhang W, Zhou C, Lei A (2014) Palladium catalysed β -selective oxidative Heck reaction of an electron-rich olefin. *Chem Commun* 50:1110–1112
54. Polshettiwar V, Hesemann P, Moreau JJE (2007) Palladium containing nanostructured silica functionalized with pyridine sites: a versatile heterogeneous catalyst for Heck, Sonogashira, and cyanation reactions. *Tetrahedron* 63:6784–6790
55. Petrucci C, Cappelletti M, Piermatti O, Nocchetti M, Pica M, Pizzo F, Vaccaro L (2015) Immobilized palladium nanoparticles on potassium zirconium phosphate as an efficient recoverable heterogeneous catalyst for a clean Heck reaction in flow. *J Mol Catal A* 401:27–34

Publisher's Note Springer Nature remains neutral with regard to jurisdictional claims in published maps and institutional affiliations.